The Advent of Biomolecular Ultrasound Imaging

Heiles, Baptiste; Terwiel, Dion; Maresca, David

DOI
10.1016/j.neuroscience.2021.03.011

Publication date
2021

Document Version
Final published version

Published in
Neuroscience

NEUROSCIENCE

REVIEW

B. Heiles et al. / Neuroscience 474 (2021) 122–133

The Advent of Biomolecular Ultrasound Imaging

Baptiste Heiles, Dion Terwiel and David Maresca*

Department of Imaging Physics, Delft University of Technology, Delft, The Netherlands

Abstract—Ultrasound imaging is one of the most widely used modalities in clinical practice, revealing human prenatal development but also arterial function in the adult brain. Ultrasound waves travel deep within soft biological tissues and provide information about the motion and mechanical properties of internal organs. A drawback of ultrasound imaging is its limited ability to detect molecular targets due to a lack of cell-type specific acoustic contrast. To date, this limitation has been addressed by targeting synthetic ultrasound contrast agents to molecular targets. This molecular ultrasound imaging approach has proved to be successful but is restricted to the vascular space. Here, we introduce the nascent field of biomolecular ultrasound imaging, a molecular imaging approach that relies on genetically encoded acoustic biomolecules to interface ultrasound waves with cellular processes. We review ultrasound imaging applications bridging wave physics and chemical engineering with potential for deep brain imaging.

Key words: acoustic biosensors, biomolecular ultrasound, functional ultrasound imaging, gas vesicles, ultrasound contrast agents, neuroimaging.

INTRODUCTION

Ultrasound imaging is used daily in clinical practice to assess the anatomical and physiological features of organs. Next to diagnostic applications in obstetrics and cardiology, we are witnessing a growing interest for ultrasound imaging in the field of neuroscience (Rabut et al., 2020).

Transcranial ultrasound Doppler has been used for decades to assess the cerebrovascular function of major arteries of the brain (Aaslid et al., 1982). In 2011, functional ultrasound neuroimaging (fUS) (Macé et al., 2011; Rabut et al., 2019) has been introduced as a breakthrough modality that relies on neurovascular coupling to map neuronal activity with a higher spatiotemporal resolution and portability than fMRI (Deffieux et al., 2018). fUS has been used to track epilepsy crises in human neonates (Demene et al., 2017) or to delineate tumor-brain interfaces in neuro-oncology patients (Imbault et al., 2017; Soloukey et al., 2020). More recently, a technique inspired by optical super-resolution named 3D ultrasound localization microscopy (ULM) has generated vascular maps of the living brain with a 30 microns resolution (Heiles, 2019). Unfortunately, these ultrasound imaging methods are not inherently sensitive to cellular and molecular processes.

To observe biological processes at the cellular scale, ultrasound engineers can now rely on endogenous, synthetic or biomolecular contrast agents (Fig. 1) as vascular or intracellular reporters (Rabut et al., 2020). Red blood cells (RBCs) are a unique cell type that can be detected with high specificity thanks to their motion. RBC motion differs significantly from collective tissue motion and induces a phase shift in ultrasound signals (Bonnefous and Pesqué, 1986) that can be captured to map blood vessels (Bercoff et al., 2011) (Fig. 1A). Lipid-shelled microbubbles (MBs) are the main class of synthetic ultrasound contrast agents (Fig. 1B). MBs scatter ultrasound more efficiently than RBCs thanks to their highly compressible gas core, and are administered intravenously to image blood perfusion (Kaul, 2008). MBs have also been engineered to target specific endothelial biomarkers (Ferrara et al., 2007). The combination of ultrasound imaging with targeted MBs is the most established molecular ultrasound imaging strategy so far. In 2014, genetically encoded acoustic biomolecules called gas vesicles (GVs) have been introduced as ultrasound analogs to the green fluorescent protein (Tsien, 1998; Shapiro et al., 2014) (Fig. 1C). GVs enable acoustic labeling of cells which opens the possibility of tracking cellular processes with ultrasound (Maresca et al., 2018b, 2018c).

*Corresponding author. Address: Lorentzweg 1, 2628 CJ Delft, The Netherlands.
E-mail address: d.maresca@tudelft.nl (D. Maresca).

Abbreviations: AM, amplitude modulation; fUS, functional ultrasound neuroimaging; GvpC, GV protein C; GVs, gas vesicles; HRF, hemodynamic response function; MBs, microbubbles; PI, pulse inversion; RBCs, Red blood cells; UDI, ultrafast Doppler imaging; ULM, ultrasound localization microscopy; VEGF, vascular endothelial growth factor.

https://doi.org/10.1016/j.neuroscience.2021.03.011

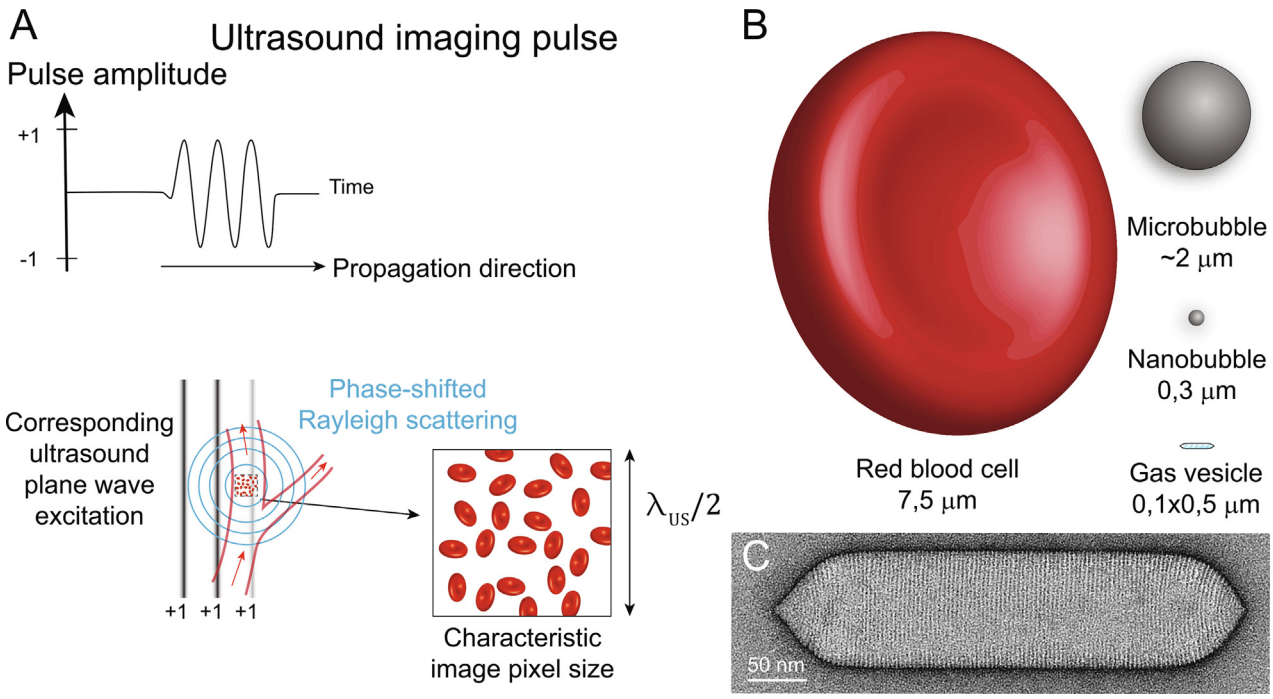

Fig. 1. Contrast agents used in ultrasound neuroimaging. **(A)** Scattering of an ultrasound imaging pulse by circulating red blood cells. **(B)** Scale comparison of endogenous, synthetic and biomolecular ultrasound contrast agents. **(C)** Transmission electron microscopy image of a single GV.

Endogenous, synthetic, and biomolecular ultrasound contrast agents enabled various molecular imaging applications such as ultrasound imaging of erythrocyte aggregation (Yu et al., 2011), ultrasound imaging of vascular endothelial growth factor (VEGF) (Wang et al., 2018), or ultrasound imaging of gene expression (Bourdeau et al., 2018; Farhadi et al., 2019). GV engineering has also led to the development of acoustic biosensors that could be used across a wide spectrum of applications (Lakshmanan et al., 2016, 2020).

This review article presents an overview of recent ultrasound technologies for deep imaging of the living brain. We cover recent ultrasound neuroimaging methods, ultrasound contrast agents used to interface with the brain, molecular imaging applications in the vascular space, and extravascular biomolecular imaging applications. Our focus is on methods to interface a penetrant form of energy – ultrasound waves – with cellular processes occurring in the brain. Light transmission based methods such as photoacoustics (Wang and Yao, 2016) are not discussed here.

RECENT ADVANCES IN ULTRASOUND NEUROIMAGING

Recent ultrasound neuroimaging methods rely exclusively on intravascular acoustic contrast (Fig. 2). Neurovascular signals are separated from the global brain ultrasound backscatter thanks to their motion or their specific frequency content. In the mammalian brain, blood flow velocities range from tens of centimeters per second in major arteries (Aaslid et al., 1982) to less than1 mm/s in capillaries supplying neurons with oxygen (Ivanov et al., 1981). At 15 MHz – a frequency often used for preclinical ultrasound imaging – the ultrasound voxel size is typically 10^6 μm^3, which contains about 100 cortical neurons (Keller et al., 2018) or 10^5 RBCs in mice (McGarry et al., 2010). Ultrasound neuroimaging is therefore mapping the dynamics of cell populations rather than individual cells (Table 1).

Mapping cerebrovascular function with ultrafast ultrasound Doppler imaging

With the introduction of high framerate plane wave ultrasound imaging, referred to as ultrafast ultrasound (Tanter and Fink, 2014), ultrasound imaging can now capture thousands of images per second. This ultrasound imaging approach was originally proposed by Bruneel et al. (1977) but only recently made possible thanks to modern multi-core computing architectures (Tanter and Fink, 2014). Instead of forming ultrasound images line by line, ultrafast ultrasound imaging relies on tilted plane wave transmissions to insonify brain tissues at kilohertz framerates (Montaldo et al., 2009).

Ultrafast ultrasound Doppler imaging (UDI) exploits these high framerates to achieve dense spatiotemporal sampling of RBC motion in tissue regions of interest. The UDI signal is a combination of blood scattering, tissue scattering, and noise. A critical problem in UDI is therefore to distinguish signal contributions arising from blood from signal contributions arising from other tissue types and noise. Recent approaches rely on spatiotemporal filtering of ultrafast ultrasound datasets (Demene et al., 2015).

Experimental comparisons have shown that UDI is 30–50 times more sensitive than conventional Doppler imaging (Macé et al., 2011; Mace et al., 2013). This

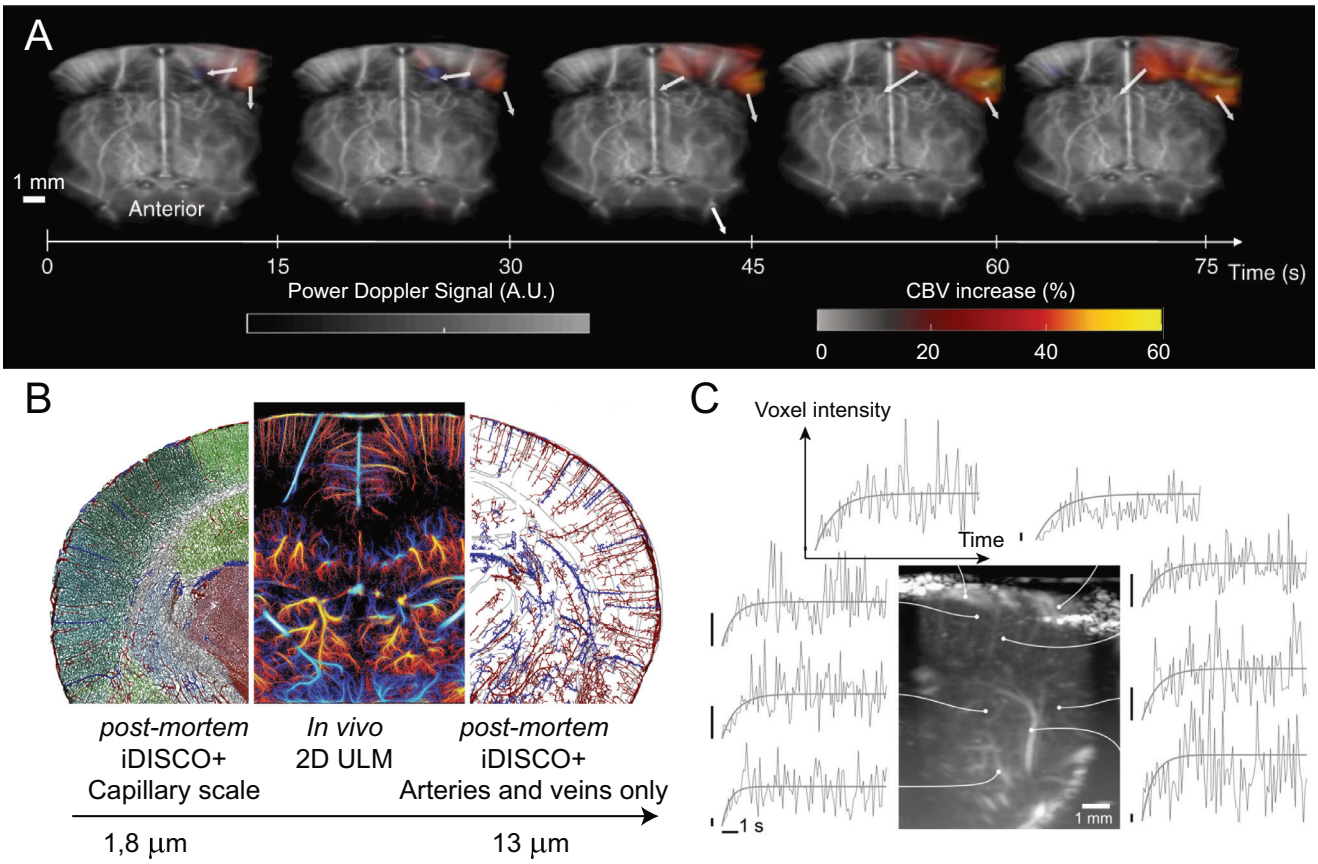

Fig. 2. Emerging ultrasound neuroimaging methods. **(A)** 4D fUS imaging of the rat brain, adapted with permission from (Rabut et al., 2019). **(B)** ULM resolution compared to that of a post-mortem tissue clearing method (iDISCO+). Adapted with permission from (Kirst et al., 2020). **(C)** Temporal variations of cerebral hemodynamics measured by a nonlinear ultrasound imaging pulse sequence. Adapted with permission from (van Raaij et al., 2012).

Table 1. Overview of non-contrast and contrast-enhanced ultrasound neuroimaging methods. x-AM, cross amplitude modulation.

Contrast-free methods	Linear contrast-enhanced methods	Nonlinear contrast-enhanced methods
fUS imaging (Rabut et al., 2019)	MB-enhanced fUS imaging (Errico et al., 2016) GV-enhanced fUS imaging (Maresca et al., 2020)	AM & PI imaging of MBs and NBs (Pellow et al., 2021) AM & PI nonlinear Doppler imaging (Tremblay-Darveau et al., 2016) x-AM imaging of GV (Maresca et al., 2018c)

increase in sensitivity is key to capture blood flow variations in smaller vessels. UDI was successfully applied in a range of medical disciplines such as rheumatology (Maresca et al., 2014), cardiology (Ekroll et al., 2015; Maresca et al., 2018a, 2018b, 2018c), stroke imaging (Hingot et al., 2020), or intensive care (Demené et al., 2018). The capacity of UDI to map flow variations in small brain vessels led to the fUS imaging breakthrough. fUS relies on neurovascular coupling that serves as an indirect readout of neural activity (like in fMRI) (Macé et al., 2011). Since 2011, fUS imaging (Fig. 2A) was reported in many animal models (Rabut et al., 2020), using experimental paradigms to study brain-wide circuits during sleep, active behavior, motor planning or recently optogenetic stimulation (Brunner et al., 2020). In a clinical setting, fUS imaging has been used to monitor neonates (Demené et al., 2014) and during tumor resection surgery (Imbault et al., 2017; Soloukey et al., 2020).

Mapping cerebrovascular anatomy with ULM

Replacing fluorophores with MB contrast agents, and relying on the imaging speed of ultrafast ultrasound, Errico et al. (Errico et al., 2015) super-resolved the rat brain vasculature with a 10 μm precision ($\lambda_{US}/10$). This technique, referred to as ULM (Couture et al., 2018) (Fig. 2B), has also been used to visualize tumors (Lin et al., 2017), kidneys (Foiret et al., 2017; Song et al., 2017a, 2017b), diabetes (Harput et al., 2018) and embryos (Song et al., 2018). 3D ULM was recently demonstrated *in vitro* (Heiles et al., 2019) and *in vivo* in the rat brain (Christensen-Jeffries et al., 2020; Heiles, 2019).

A critical parameter in ULM is the ability to detect individual MBs. Initially, a frame to frame subtraction or a rolling background technique was used to subtract static echoes (Siepmann et al., 2011; Christensen-Jeffries et al., 2015). This technique is hardly applicable

in vivo because tissue motion can be important and out-of-plane, leading to inaccurate MB localization (Heiles et al., 2019). Spatiotemporal filters have been successfully used in this context as well to separated MB signals from tissue clutter (Desailly et al., 2017). Pixel oriented filtering methods such as the non-local means technique are also providing good results (Song et al., 2018).

Current ULM methods rely on MB motion. If MBs are targeted to endothelial biomarkers or stopped by a vascular occlusion, their ULM detection is no longer possible. This problem can be solved by relying on the unique nonlinear frequency content of MB echoes rather than on MB motion. Nonlinear ultrafast ultrasound imaging of MBs has been demonstrated (Couture et al., 2012; Tremblay-Darveau et al., 2016; Muleki-Seya et al., 2020) and lends itself well to ULM processing (Zhao et al., 2020). In this context, special attention must be given to MB destruction, especially when mapping targeted MBs for molecular imaging applications.

Mapping blood perfusion with nonlinear ultrasound pulse sequences

Several ultrasound pulse sequences dedicated to MB detection have been reported over the years. In neuroscience, van Raaij et al. (2011, 2012) showed that high-frequency nonlinear ultrasound imaging of MBs could capture rat brain activity evoked by forepaw stimulation (Fig. 2C).

A first class of pulse sequences relies on amplitude modulation (AM) of ultrasound pulses transmitted in tissues. Low amplitude ultrasound pulses elicit a linear response from MB and tissues, whereas high amplitude ultrasound pulses elicit a nonlinear response from MBs but not from tissues. The AM response of MBs is unique and differs from that of tissue. Ultrafast AM imaging has been used for characterization of kidney and tumor perfusion (Tremblay-Darveau et al., 2016).

A second class of ultrasound pulse sequences relies on the pulse inversion (PI) of ultrasound imaging pulses. In PI imaging, pairs of phase inverted pulses are transmitted into tissues and the echoes recorded are subsequently summed. This process retains nonlinear signatures that are unique to MBs circulating in tissues. Ultrafast PI imaging has been used to study blood perfusion (Leow et al., 2015).

A drawback of nonlinear ultrasound pulse sequences is their susceptibility to nonlinear propagation artifacts that misclassify tissues as contrast agents (ten Kate et al., 2012; Maresca et al., 2017). This occurs when ultrasound waves travel through large inclusions of nonlinear contrast agents. Imaging methods based on cross-propagating plane waves are currently investigated and have shown to significantly reduce nonlinear propagation artifacts (Maresca et al., 2018c).

ENDOGENOUS, SYNTHETIC AND BIOMOLECULAR ULTRASOUND CONTRAST AGENTS

Ultrasound waves are backscattered by microscale structures such as cells or ultrasound contrast agents. Individual particles with dimensions below a tenth of the wavelength ($\lambda_{US}/10$) are referred to as Rayleigh scatterers (Helfield, 2019) and their reflective power is characterized by the scattering cross section σ_{Rs},

$$\sigma_{Rs} \propto V_{Rs}^2 f_{US}^4 \left(\left(\frac{\kappa_{Rs} - \kappa_0}{\kappa_0} \right)^2 + 3 \left(\frac{\rho_{Rs} - \rho_0}{2\rho_{Rs} + \rho_0} \right)^2 \right) \quad (1)$$

with f_{US} the ultrasound wave frequency, V_{Rs} the volume of the Rayleigh scatterer, κ_{Rs} and κ_0 the compressibility of the scatterer and of the surrounding medium respectively, ρ_{Rs} and ρ_0 the mass density of the scatterer and of the surrounding medium respectively.

Eq. (1) states that microscale particles exhibiting a density and/or compressibility contrast with surrounding tissue scatter ultrasound waves (Fig. 1A). In addition, σ_{Rs} scales with ultrasound frequency to the power 4. An example is RBC contrast which is hardly visible at 1 MHz but easily detectable at 10 MHz and above (Szabo, 2004).

Last, it is worth noting that Rayleigh scattering can also arise from structural inhomogeneities within cells such as genetically encoded GVs (Sehgal and Greenleaf, 1984; Bourdeau et al., 2018; Farhadi et al., 2019).

RBCs as indirect reporters of neuronal activity

While the acoustic contrast arising from RBCs does not inform directly on cellular or molecular events, it can measure functional hyperemia induced by neurovascular coupling (Boido et al., 2019). In a recent study, Aydin et al. (Aydin et al., 2020) reported that functional hyperemia measured with fUS imaging is a robust reporter of underlying neuronal calcic activity. The hemodynamic response function (HRF) of the brain typically lags ~2 s behind the electric response (Masamoto and Kanno, 2012). In fUS imaging, the HRF has been modeled as a gamma-distribution function with no post-stimulus undershoot (Aydin et al., 2020).

It is therefore possible to exploit ultrasound backscattering induced by RBC motion to capture neural activity with ultrasound. However, that measure is indirect.

Synthetic MBs and nanobubbles

MBs are the first and most widespread ultrasound contrast agents. Early developments aimed at controlling their scattering power as well as their stability (Ophir and Parker, 1988). Modern synthetic MBs are stable enough to pass through the heart and lungs, and their *in vivo* lifetime allows for multiple recirculations which lengthens the diagnostic window (Frinking et al., 2020).

To stabilize MBs, a majority of them are now coated with a phospholipid layer, and their gas core is made of perfluorinated gases such as sulfur hexafluoride (Schneider et al., 1995), perfluoropropane (Unger et al., 1994), or perfluorobutane (Schneider et al., 1997, 2011). More than a dozen agents have now been commercialized with various technologies.

Commercial MB diameters range from 0.5 to 10 μm (Frinking et al., 2020) which lets them circulate in most

vessels after intravenous injection (Fig. 1B). The scattering power of MBs is directly linked to their size and ability to resonate at medical ultrasound frequencies (Helfield, 2019). Recently, monodisperse MB size distributions have triggered interest as these can boost MB echogenicity further (Segers et al., 2018).

MBs are too large to extravasate (Ferrara et al., 2009; Moestue et al., 2012). In healthy vasculature, particles above 7 nm cannot pass through endothelial tight junctions (Hobbs et al., 1998). In leaky cancer vasculature, particles as large as 380–780 nm were shown to extravasate (Maeda et al., 2009). This consideration triggered the development of nanobubble (NB) ultrasound contrast agents for cancer imaging (Gao et al., 2017; Hamano et al., 2019) and drug delivery (Song et al., 2017a, 2017b; de Leon et al., 2019; Pellow et al., 2021).

Synthetic MBs can also be engineered to adhere to vascular biomarkers, creating the possibility for molecular ultrasound imaging of endothelial function. By adding targeting ligands to their shell, such as peptides, proteins, polymers, antibodies or aptamers, targeted MBs capable of sensing inflammation (with ICAM-1, VCAM-1, E-selectin, P-selectin) (Fokong et al., 2013; Li et al., 2019), angiogenesis (with $\alpha_v\beta_3$ integrin, VEGF, VEGFR2, endoglin) (Willmann et al., 2008; Pochon et al., 2010; Alzaraa et al., 2012) or thrombosis (cRGD) (Schumann et al., 2002; Wang et al., 2012) have been created.

Increasing the sensitivity of molecular ultrasound imaging with monodisperse MBs would be particularly valuable as just a fraction of targeted MBs end up binding to endothelial markers (Talu et al., 2007; Shih et al., 2013). Finally, Nakatsuka et al. (2012) demonstrated that it was possible to engineer MBs that become reflective only when levels of thrombin are significant but remain dormant in normal physiological conditions.

Acoustic biomolecules

The adoption of molecular ultrasound imaging based on MBs remains limited because of MB size, intravascular confinement, and short MB half-life in circulation (Kaufmann and Lindner, 2007; Wang et al., 2018).

Recently, GVs were introduced as a new class of genetically encoded ultrasound contrast agents that have the potential to become the ‘‘GFP for ultrasound” (Rabut et al., 2020). GVs are ancient hollow protein nanostructures evolved as motility devices by aquatic microorganisms to regulate their buoyancy (Fig. 3A). In 2014, Shapiro et al. (2014) realized that the gas content of GVs would make them bright in ultrasound images. The GV nanostructure consists of two proteins. GV protein A (GvpA) forms the spindle-shaped backbone structure and GV protein C (GvpC) binds externally to GvpA and stiffens the assembled GV (Walsby, 1994).

Both linear and nonlinear ultrasound imaging of GVs was reported in literature (Shapiro et al., 2014; Cherin et al., 2017; Yang et al., 2017). Nonlinear GV scattering is thought to arise from large GV shell deformations referred to as buckling (Maresca et al., 2017). At medical ultrasound frequencies, this buckling behavior occurs at pressures above a few hundreds of kPa and makes GVs particularly suited for AM ultrasound imaging (Maresca et al., 2017).

Thanks to their biogenic origin, GVs lend themselves to molecular and genetic engineering (Fig. 3). The acoustic properties of GVs have been successfully manipulated by altering GvpC binding to GvpA. Complete GvpC removal was shown to weaken GVs and increase their nonlinear scattering (Lakshmanan et al., 2016; Maresca et al., 2017). GvpC removal is also lowering GV collapse pressue. This characteristic was leveraged to engineer acoustic reporters with distinct acoustic collapse pressures and used for multiplexed imaging (Lakshmanan et al., 2016). Specific biomarkers can also be bound to to the outer wall of GVs, following the example of targeted MBs. In summary, GvpC provides a convenient handle for GV shell functionalization.

MOLECULAR ULTRASOUND IMAGING USING VASCULAR AGENTS

Targeted MBs as acoustic reporters of endothelial function

Many vascular inflammation diseases and types of cancer are characterized by differential expression of endothelial biomolecules. Targeted MBs have been successfully used to bind to multiple membrane proteins such as P- and E-selectin, VCAM-1 and ICAM-1, locally enhancing imaging contrast in diseased areas (Hamilton et al., 2004; Kaufmann and Lindner, 2007; Chadderdon et al., 2014).

In practice, ultrasound imaging with targeted MBs requires a significant difference in concentration between bound and unbound MBs. A 5–10 min window after intravenous injection is enough for the reticuloendothelial system to clear non-functionalized MBs from the bloodstream. MB clearance is also in part due to acoustic collapse or gas diffusion through the MB phospholipid shell (Kosareva et al., 2020). A vast majority of methods for discerning bound and freely circulating MBs rely on destruction-replenishment strategies. In destruction-replenishment methods, MBs are first destroyed using a high-intensity ultrasound pulse. The subsequent signal is assumed to be arising from freely-circulating MBs and can be subtracted from the initial signal that accounts for both bound and unbound MBs (Abou-Elkacem et al., 2015).

Molecular ultrasound imaging using targeted MBs has been recently combined with ULM to co-localize vascular anatomy and vascular markers of angiogenesis (Zhao et al., 2020) (Fig. 4A). This promising multimodal approach could be used to study longitudinal cancer development and vascular remodeling in living organisms.

GV-enhanced hemodynamic fUS imaging

GVs were recently investigated as hemodynamic enhancers for sensitive transcranial fUS imaging in mice (Maresca et al., 2020) (Fig. 4B). This study constitutes a first step towards biomolecular fUS imaging of neural activity. Purified GVs were used as linearly scattering

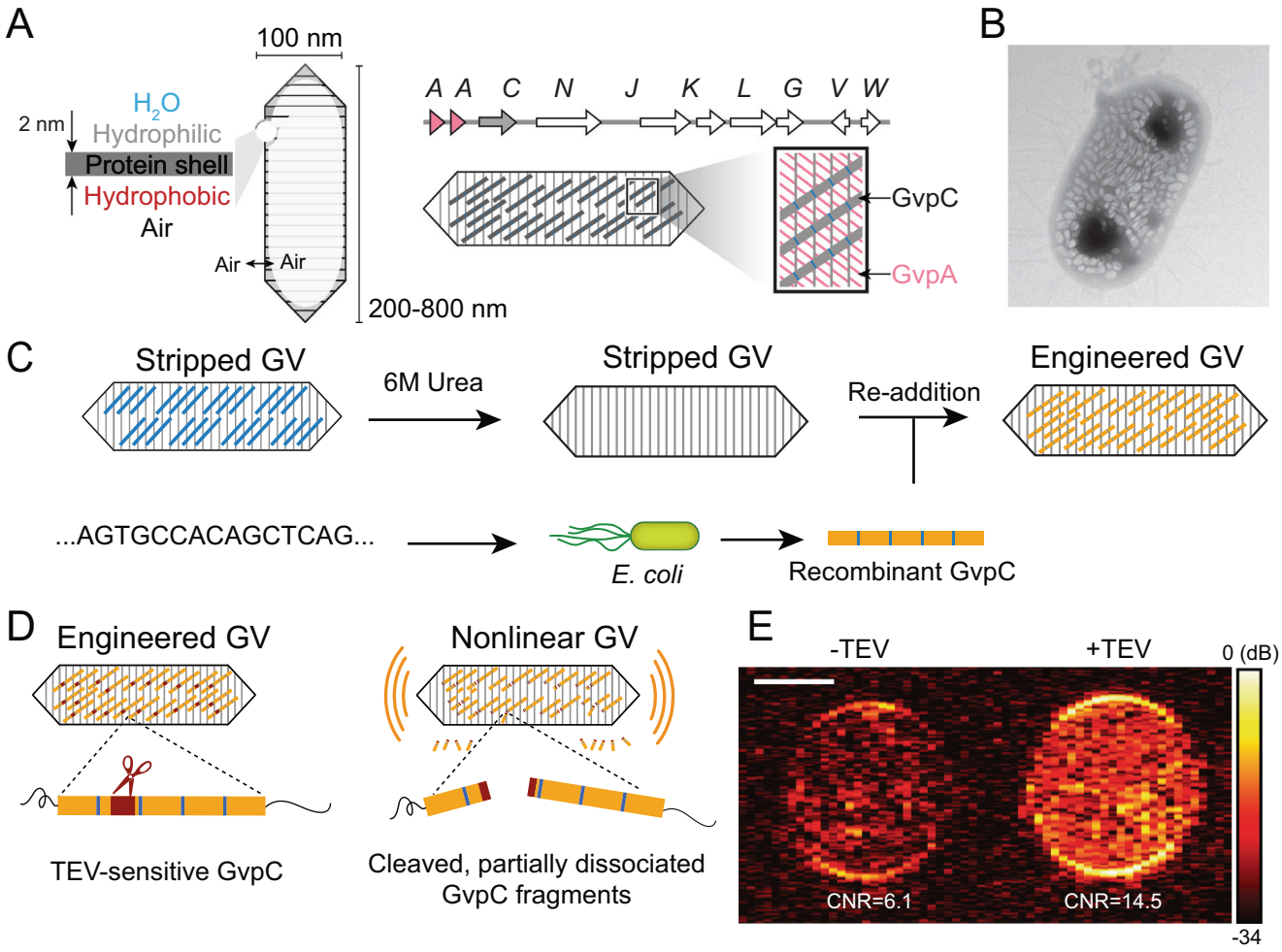

Fig. 3. GV engineering . **(A)** GV hollow protein nanostructure, gene cluster encoding GVs and surface arrangement of the GV shell proteins GvpA and GvpC. Adapted with permission from (Maresca et al., 2018b). **(B)** Heterologous expression of gas vesicles in *E. coli*. Adapted with permission from (Bourdeau et al., 2018). **(C)** GvpC bioengineering pipeline, adapted with permission from (Maresca et al., 2018b). **(D)** Design of an acoustic biosensor of Tobacco Etch Virus (TEV) protease activity. Adapted with permission from (Lakshmanan et al., 2020). **(E)** Nonlinear ultrasound imaging of acoustic biosensors of TEV activity. Scale bar = 1 mm. Adapted with permission from (Lakshmanan et al., 2020).

nanoparticles circulating alongside RBCs, increasing the overall blood backscatter and raising the sensitivity of Doppler methods.

A first finding was that thanks to their nanoscale, inherent stability, and large numbers in circulation, GVs-enhanced UDI could measure slow flow velocities more accurately than conventional UDI and MB-enhanced UDI (Maresca et al., 2020). One possible explanation is that unlike MBs, GVs are dominated by Stokes drag over other forces such as buoyancy. The capacity of GVs to enhance Doppler signals down to 50 μm/s flow velocities is critical to map the neurovascular coupling in the smallest vascular compartments (Boido et al., 2019).

A second finding was that intravenous bolus injection of GVs did enhance ultrafast Doppler signals in the mouse brain. While the peak enhancement provided by GVs was inferior to that of MBs (+34% compared to baseline level for GVs and +149% for MBs), GVs yielded a significantly smoother Doppler signal enhancement (the mean variance of the fast time fluctuation of the GV-enhanced Doppler signal was 0.8% compared to 4.5% for the MB-enhanced Doppler signal).

A third finding was that bolus injections of GVs provided a pseudo-steady transcranial enhancement of fUS signals over the course of 4 minutes in mice, whereas bolus injections of MBs deteriorated the quality of brain activity maps. In the future, a comparison of different modes of administration (bolus versus infusion) and a broader range of doses would help optimize this imaging approach.

It is worth noting that in contrast-free fUS imaging, the percent change in fUS signals at 15 MHz is lower in mice (~5%) (Brunner et al., 2020) than in rats (~15%) (Rabut et al., 2019) for a given brain stimulation protocol (e.g. whisker stimulation). This might be due to differences in RBC volume – 45.5 μm^3 in laboratory mice (de Jong et al., 2001) versus 60.7 μm^3 in laboratory rats (Garcia et al., 2012). This justifies the need for methods capable

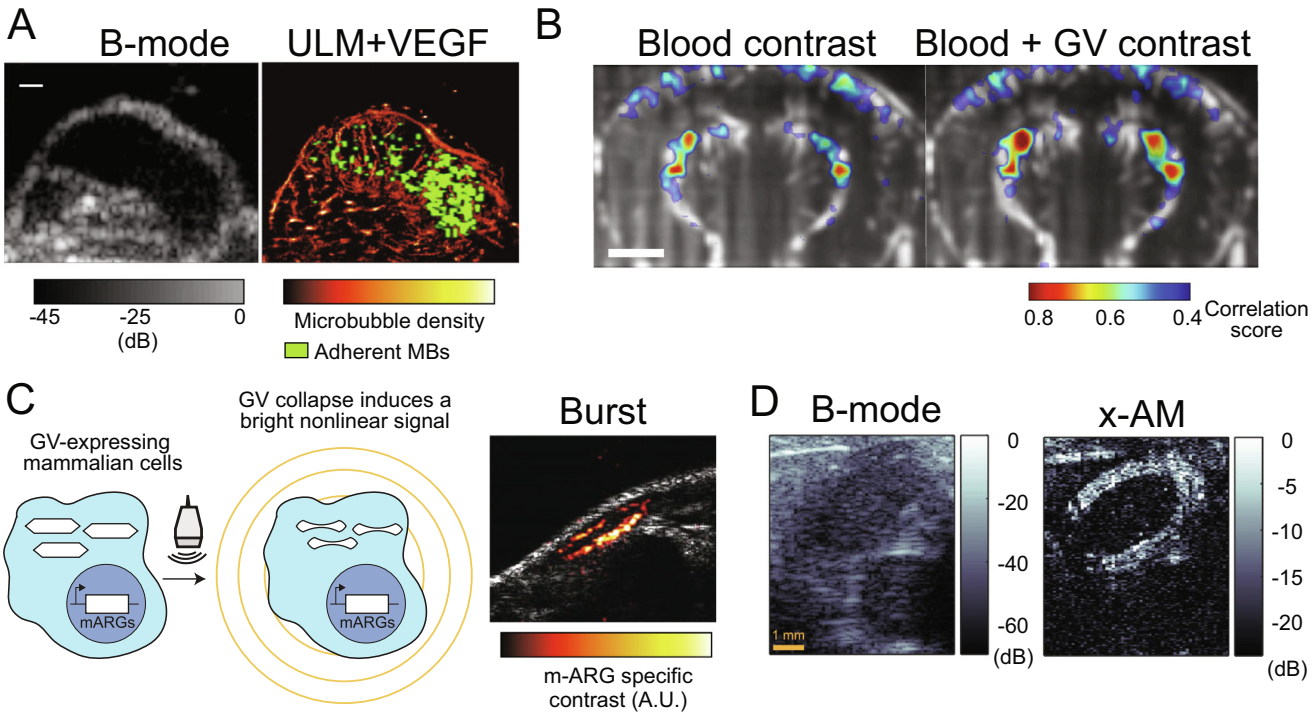

Fig. 4. Biomolecular ultrasound imaging in mouse models. **(A)** Molecular ultrasound imaging of VEGF expression in a mouse tumor model using targeted MBs, co-registered with ULM imaging of vascular anatomy . Scale bar = 1 mm. Adapted with permission from (Zhao et al., 2020). **(B)** Transcranial GV-enhanced fUS imaging of the mouse brain. Scale bar = 1 mm. Adapted with permission from (Maresca et al., 2020). **(C)** Ultrasound imaging of gene expression in a mouse tumor model using a GV-collapse based approach. Image width 9 mm. Adapted with permission from (Farhadi et al., 2019). **(D)** Nondestructive x-AM imaging reveals the presence of GVs in the gastrointestinal tract of a mouse. Adapted with permission from (Maresca et al., 2018c).

of enhancing fUS sensitivity in mice. The benefit of GVs at lower ultrasound frequencies and in larger brains remains to be demonstrated. In any case, efforts to engineer brighter GVs will be beneficial across medical ultrasound frequencies (Hurt et al., 2021).

Together these results demonstrated that GVs could become a preferred contrast agent for fUS imaging thanks to their noise-free enhancement of fUS signals across a wide range of cerebral blood flow velocities.

Imaging with engineered RBC contrast

An interesting strategy to couple molecular events to hemodynamic fUS imaging could be to artificially trigger vasodilatory responses in the brain using vasodilating peptides (Desai et al., 2016; Ohlendorf et al., 2020). Using fMRI, Desai et al. showed that nanomolar concentrations of the cgrp peptide induced larger cerebral flood flow variations than neurovascular coupling. Since fUS imaging measures local blood flow variations in the brain, molecular ultrasound imaging combining fUS and vasoactive peptides could be envisioned.

Another interesting chemical engineering approach consists of using RBC membranes to "hide" ultrasound contrast agents from the immune system (Dhanaliwala and Hossack, 2012) and increase the contrast agent circulation time (Hu et al., 2011). RBCs can circulate in the bloodstream for several months whereas the lifetime of MB circulation is of the order of 10 min and prevents longitudinal experiments. Contrast-enhanced transcranial fUS imaging methods would greatly benefit from long circulating contrast agents (Errico et al., 2016; Maresca et al., 2020).

BIOMOLECULAR ULTRASOUND IMAGING APPLICATIONS

Ultrasound imaging of gene expression

GVs are the first genetically encoded acoustic biomolecules and could become the "GFP for Ultrasound" (Rabut et al., 2020). GVs are encoded by highly conserved genetic clusters of 8–12 genes in microorganisms such as *Anabaena flos-aquae* (Maresca et al., 2018b). Two of these genes encode for the structural proteins GvpA and GvpC that are the main constituents of GV nanostructures. Fully assembled GVs present a 2 nm-thick shell made of periodic repeats of the single protein GvpA which is further reinforced with the external scaffold protein GvpC.

In 2018, Bourdeau et al. (Bourdeau et al., 2018) demonstrated heterologous expression of GVs in *Escherichia coli* (*E. coli*) (Fig. 3B) and *Salmonella typhimurium*, making these engineered cells visible with ultrasound imaging. In addition, Bourdeau et al. reported ultrasound imaging of bacteria in the gastrointestinal (GI) tract of mice, a first demonstration of cell tracking with ultrasound. Interestingly, GV-expression in E. Coli is also creating the possibility for high-throughput screening of engineered

echogenic bacterial phenotypes (Bourdeau et al., 2018; Hurt et al., 2021).

In 2019, Farhadi et al. (2019) reported genetic expression of GVs in mammalian cells. Their study showed that acoustic contrast arising from GVs and occupying less than 0.1% of the cytoplasm could be detected using a destructive template-based ultrasound imaging sequence named BURST. Using this approach, they reported depth-resolved ultrasound imaging of GV expression in a subcutaneous tumor model (Fig. 4C). In the future, ultrasound imaging of mammalian acoustic reporter genes (mARGs) using nondestructive methods such as cross AM (Maresca et al., 2018c) should emerge (Fig. 4D).

The development of mARGs is still in its infancy and research efforts are needed to facilitate targeted GV expression in various cell-types using viral vectors. In neuroscience, a potential application could be to drive GV-expression with neural activity-dependent promoters such as Arc, fos or E-SARE (DeNardo and Luo, 2017) to observe time integrated neural responses in the brain. A second exciting route is to engineer GVs into acoustic intracellular sensors to study dynamic cellular processes deep into brain tissues.

Acoustic biosensors for deep molecular ultrasound imaging

Following the discovery of GFP, fluorescent proteins were further engineered into genetically-encoded indicators to investigate biological processes at the cellular scale. In neuroscience, genetically encoded calcium and voltage indicators are now established tools to study cognition in animal models.

Lakshmanan et al. (2016) showed that the acoustic response of GVs could be shifted from linear to nonlinear by removing GvpC (Fig. 3C), a first critical step towards the development of an acoustic biosensor. In 2020, they reported the first genetically encoded acoustic biosensor with tunable nonlinear constrast in response to protease activity (Lakshmanan et al., 2020) (Fig. 3D). To do so, they inserted a short recognition sequence for the model Tobacco Etch Virus (TEV) endopeptidase into one of the GvpC repeats. They observed that GVs covered with TEV-sensitive GvpC were weakened in the presence of TEV, which led to increased nonlinear ultrasound scattering (Fig. 3E). Similar results were obtained for two other acoustic biosensor designs, one based on the calcium-activated calpain protease, and the other on a degradation tag appended to the C-terminus of GvpC (model proteosome ClpXp). These acoustic biosensors were successfully expressed in probiotic bacteria and imaged in the mouse GI tract.

In neuroscience, proteases are involved in various aspects of neuropathophysiology. For example, intracellular proteases such as calpain and caspases get involved in neuronal dysfunction in Alzheimer's disease. A current limitation is that acoustic biosensors based on GvpC degradation are not reversible and cannot report on dynamic intracellular processes. The feasibility of fast and reversible acoustic biosensors conceptually similar to GCamP (Lin and Schnitzer, 2016) remains an open research question.

Ultrasound imaging of phagolysosomal function

Next to genetic expression of mARGs, purified GVs can be used as an injectable to report on cellular activity. In a proof-of-concept study, Ling et al. (2020) used GVs to image liver macrophage phagolysosomal function with ultrasound. After intravenous injection, purified GVs get cleared from the bloodstream by liver macrophages that recognize them as foreign particles. Next, phagocytosed GVs undergo lysosomal degradation. This process was monitored by Ling et al. using two different ultrasound imaging modes. UDI was used to track GV circulation in brain vessels over time. A sharp increase in UDI intensity was observed 100 s after injection before decreasing over time due to GV retention in the liver. The GV circulation half-life was equal to 230 s. In parallel to UDI, the accumulation of GVs in liver macrophages was monitored using AM ultrasound imaging. AM signals peaked 10 minutes after injection, before decreasing due to lysosomal degradation of GVs. Together, these results showed that ultrasound imaging of phagocytosis and lysosomal degradation rates could be used to diagnose healthly versus diseased liver states in humans.

In neuroscience, purified GVs could be used as an injectable to report on cerebrovascular afflictions such as ischemia–reperfusion injuries, atherosclerosis, or brain tumors.

OUTLOOK AND OPPORTUNITIES IN NEUROSCIENCE

The field of biomolecular ultrasound imaging was born in 2014 with the introduction of GVs as genetically encoded ultrasound contrast agents. GVs have now been used as acoustic reporters genes in bacteria and mammalian cells, engineered into acoustic biosensors of protease activity, and vascular reporters for transcranial functional ultrasound neuroimaging or imaging of macrophage phagolysosomal function.

Next to the introduction of GVs, the field of ultrasound neuroimaging has witnessed major developments. In 2011 (Macé et al., 2011), functional ultrasound neuroimaging was established as a breakthrough modality that can map brain activity where fMRI fails: in freely moving animals, human neonates, and during intraoperative brain surgery. In 2015 (Errico et al., 2015), ULM was reported as a super-resolution method capable of mapping the whole brain-wide vasculature of living mammals with a 10 μm resolution. In 2018 (Maresca et al., 2018c), a new nonlinear ultrasound pulse sequence enabled depth-resolved, nondestructive tracking of GVs in the GI tract (Fig. 4D). The combination of ultrasound neuroimaging with endongenous, synthetic and biomolecular ultrasound contrast agents will undoubtedly create new opportunities for deep molecular imaging of the living mammalian brain.

Clinical use of biomolecular ultrasound technologies is far ahead, but two translational paths can be envisioned. The first is cell-based. Genetically modified cell agents

such as CAR T cells are already sent in the human body to fight cancer (Brentjens et al., 2013). These cells could augmented with the capacity to produce their own acoustic contrast and enable ultrasound monitoring of immune cell therapy. From a regulatory point of view, potential immune responses to GVs - bacteria-derived proteins – will need to be investigated. The second path consists in using GVs as purified nanoparticles administered intravenously. A potential application could be to sense cancer microenvironments with acoustic biosensors. Here again, future studies must be conducted to investigate potential immune reactions.

Bridging the fields of chemical engineering and acoustics, biomolecular ultrasound imaging will certainly lead to a wave of discoveries in neuroscience.

ACKNOWLEDGEMENTS

The authors thank Sefan Huber and Arjen Jakobi for assistance with TEM imaging of gas vesicles. Related research in the Maresca Laboratory is supported by the 4TU Precision Medicine Program, the Medical Delta Ultrafast Heart & Brain Program, and the Dutch Research Council NWO (Award No STU.019.021).

REFERENCES

Aaslid R, Markwalder TM, Nornes H (1982) Noninvasive transcranial Doppler ultrasound recording of flow velocity in basal cerebral arteries. J Neurosurg 57:769–774.

Abou-Elkacem L, Bachawal SV, Willmann JK (2015) Ultrasound molecular imaging: Moving toward clinical translation. Eur J Radiol 84:1685–1693.

Alzaraa A, Gravante G, Chung WY, Al-Leswas D, Bruno M, Dennison AR, Lloyd DM (2012) Targeted microbubbles in the experimental and clinical setting. Am J Surg 204:355–366.

Aydin A-K, Haselden WD, Goulam Houssen Y, Pouzat C, Rungta RL, Demené C, Tanter M, Drew PJ, Charpak S, Boido D (2020) Transfer functions linking neural calcium to single voxel functional ultrasound signal. Nat Commun 11:2954.

Bercoff J, Montaldo G, Loupas T, Savery D, Mézière F, Fink M, Tanter M (2011) Ultrafast compound Doppler imaging: providing full blood flow characterization. IEEE Trans Ultrason Ferroelectr Freq Control 58:134–147.

Boido D, Rungta RL, Osmanski B-F, Roche M, Tsurugizawa T, Le Bihan D, Ciobanu L, Charpak S (2019) Mesoscopic and microscopic imaging of sensory responses in the same animal. Nat Commun 10:1110.

Bonnefous O, Pesqué P (1986) Time domain formulation of pulse-Doppler ultrasound and blood velocity estimation by cross correlation. Ultrason Imaging 8:73–85.

Bourdeau RW, Lee-Gosselin A, Lakshmanan A, Farhadi A, Kumar SR, Nety SP, Shapiro MG (2018) Acoustic reporter genes for noninvasive imaging of microorganisms in mammalian hosts. Nature 553:86–90.

Brentjens RJ, Davila ML, Riviere I, Park J, Wang X, Cowell LG, Bartido S, Stefanski J, et al. (2013), CD19-targeted T cells rapidly induce molecular remissions in adults with chemotherapy-refractory acute lymphoblastic leukemia. Sci Transl Med 5:177ra138-177ra138.

Bruneel C, Torguet R, Rouvaen KM, Bridoux E, Nongaillard B (1977) Ultrafast echotomographic system using optical processing of ultrasonic signals. Appl Phys Lett 30:371–373.

Brunner C, Grillet M, Sans-Dublanc A, Farrow K, Lambert T, Macé E, Montaldo G, Urban A (2020) A platform for brain-wide volumetric functional ultrasound imaging and analysis of circuit dynamics in awake mice. Neuron 108:861–875.e867.

Chadderdon SM, Belcik JT, Bader L, Kirigiti MA, Peters DM, Kievit P, Grove KL, Lindner JR (2014) Proinflammatory endothelial activation detected by molecular imaging in obese nonhuman primates coincides with onset of insulin resistance and progressively increases with duration of insulin resistance. Circulation 129:471–478.

Cherin E, Melis JM, Bourdeau RW, Yin M, Kochmann DM, Foster FS, Shapiro MG (2017) Acoustic behavior of halobacterium salinarum gas vesicles in the high-frequency range: experiments and modeling. Ultrasound Med Biol 43:1016–1030.

Christensen-Jeffries K, Browning RJ, Tang M-X, Dunsby C, Eckersley RJ (2015) In vivo acoustic super-resolution and super-resolved velocity mapping using microbubbles. IEEE Trans Med Imaging 34:433–440.

Christensen-Jeffries K, Couture O, Dayton PA, Eldar YC, Hynynen K, Kiessling F, O'Reilly M, Pinton GF, Schmitz G, Tang M-X, Tanter M, van Sloun RJG (2020) Super-resolution ultrasound imaging. Ultrasound Med Biol 46(4):865–891.

Couture O, Fink M, Tanter M (2012) Ultrasound contrast plane wave imaging. IEEE Trans Ultrason Ferroelectr Freq Control 59:6373790.

Couture O, Hingot V, Heiles B, Muleki-Seya P, Tanter M (2018) Ultrasound localization microscopy and super-resolution: A state of the art. IEEE Trans Ultrason Ferroelectr Freq Control 65:1304–1320.

de Jong K, Emerson RK, Butler J, Bastacky J, Mohandas N, Kuypers FA (2001) Short survival of phosphatidylserine-exposing red blood cells in murine sickle cell anemia. Blood 98:1577–1584.

de Leon AI, Perera R, Hernandez C, Cooley M, Jung O, Jeganathan S, Abenojar E, Fishbein G, Sojahrood AJ, Emerson CC, Stewart PL, Kolios MC, Exner AA (2019) Contrast enhanced ultrasound imaging by nature-inspired ultrastable echogenic nanobubbles. Nanoscale 11:15647–15658.

Deffieux T, Demene C, Pernot M, Tanter M (2018) Functional ultrasound neuroimaging: a review of the preclinical and clinical state of the art. Curr Opin Neurobiol 50:128–135.

Demene C, Baranger J, Bernal M, Delanoe C, Auvin S, Biran V, Alison M, Mairesse J, et al. (2017), Functional ultrasound imaging of brain activity in human newborns. Sci Transl Med 9.

Demene C, Deffieux T, Pernot M, Osmanski B-F, Biran V, Gennisson J-L, Sieu L-A, Bergel A, Franqui S, Correas J-M, Cohen I, Baud O, Tanter M (2015) Spatiotemporal clutter filtering of ultrafast ultrasound data highly increases doppler and fultrasound sensitivity. IEEE Trans Med Imaging 34:2271–2285.

Demené C, Maresca D, Kohlhauer M, Lidouren F, Micheau P, Ghaleb B, Pernot M, Tissier R, Tanter M (2018) Multi-parametric functional ultrasound imaging of cerebral hemodynamics in a cardiopulmonary resuscitation model. Sci Rep 8:16436.

Demené C, Pernot M, Biran V, Alison M, Fink M, Baud O, Tanter M (2014) Ultrafast doppler reveals the mapping of cerebral vascular resistivity in neonates. J Cereb Blood Flow Metab 34:1009–1017.

DeNardo L, Luo L (2017) Genetic strategies to access activated neurons. Curr Opin Neurobiol 45:121–129.

Desai M, Slusarczyk AL, Chapin A, Barch M, Jasanoff A (2016) Molecular imaging with engineered physiology. Nat Commun 7:13607.

Desailly Y, Tissier A-M, Correas J-M, Wintzenrieth F, Tanter M, Couture O (2017) Contrast enhanced ultrasound by real-time spatiotemporal filtering of ultrafast images. Phys Med Biol 62:31–42.

Dhanaliwala K, Hossack (2012), Microbubble-loaded red blood cells to produce acoustically active ghosts. 17th European Symposium on Ultrasound Contrast Imaging 38-40.

Ekroll IK, Voormolen MM, Standal O-V, Rau JM, Lovstakken L (2015) Coherent compounding in doppler imaging. IEEE Trans Ultrason Ferroelectr Freq Control 62:1634–1643.

Errico C, Osmanski B-F, Pezet S, Couture O, Lenkei Z, Tanter M (2016) Transcranial functional ultrasound imaging of the brain using microbubble-enhanced ultrasensitive Doppler. NeuroImage 124:752–761.

Errico C, Pierre J, Pezet S, Desailly Y, Lenkei Z, Couture O, Tanter M (2015) Ultrafast ultrasound localization microscopy for deep super-resolution vascular imaging. Nature 527:499–502.

Farhadi A, Ho GH, Sawyer DP, Bourdeau RW, Shapiro MG (2019) Ultrasound imaging of gene expression in mammalian cells. Science (New York, NY) 365(6460):1469–1475.
Ferrara K, Pollard R, Borden M (2007) Ultrasound microbubble contrast agents: fundamentals and application to gene and drug delivery. Annu Rev Biomed Eng 9:415–447.
Ferrara KW, Borden MA, Zhang H (2009) Lipid-shelled vehicles: engineering for ultrasound molecular imaging and drug delivery. Acc Chem Res 42:881–892.
Foiret J, Zhang H, Ilovitsh T, Mahakian L, Tam S, Ferrara KW (2017) Ultrasound localization microscopy to image and assess microvasculature in a rat kidney. Sci Rep 7:13662.
Fokong S, Fragoso A, Rix A, Curaj A, Wu Z, Lederle W, Iranzo O, Gätjens J, Kiessling F, Palmowski M (2013) Ultrasound molecular imaging of E-selectin in tumor vessels using poly n-butyl cyanoacrylate microbubbles covalently coupled to a short targeting peptide. Invest Radiol 48:843–850.
Frinking P, Segers T, Luan Y, Tranquart F (2020) Three decades of ultrasound contrast agents: a review of the past, present and future improvements. Ultrasound Med Biol 46:892–908.
Gao Y, Hernandez C, Yuan H-X, Lilly J, Kota P, Zhou H, Wu H, Exner AA (2017) Ultrasound molecular imaging of ovarian cancer with CA-125 targeted nanobubble contrast agents. Nanomedicine: Nanotechnology. Biol Med 13:2159–2168.
Garcia JS, Pinheiro J, Hooper CS, Simões RO, Ferraz JS, Maldonado A (2012) Haematological alterations in Rattus norvegicus (Wistar) experimentally infected with Echinostoma paraensei (Trematoda: Echinostomatidae). Exp Parasitol 131:300–303.
Hamano N, Kamoshida S, Kikkawa Y, Yano Y, Kobayashi T, Endo-Takahashi Y, Suzuki R, Maruyama K, Ito Y, Nomizu M, Negishi Y (2019) Development of antibody-modified nanobubbles using Fc-region-binding polypeptides for ultrasound imaging. Pharmaceutics 11:283.
Hamilton AJ, Huang S-L, Warnick D, Rabbat M, Kane B, Nagaraj A, Klegerman M, McPherson DD (2004) Intravascular ultrasound molecular imaging of atheroma components in vivo. J Am Coll Cardiol 43:453–460.
Harput S, Christensen-Jeffries K, Brown J, Li Y, Williams KJ, Davies AH, Eckersley RJ, Dunsby C, Tang M-X (2018) Two-stage motion correction for super-resolution ultrasound imaging in human lower limb. IEEE Trans Ultrason Ferroelectr Freq Control 65:803–814.
Heiles B (2019) 3D ultrasound localization microscopy. PSL Research University.
Heiles B, Correia M, Hingot V, Pernot M, Provost J, Couture O (2019) Ultrafast 3D ultrasound localization microscopy using a 32x32 matrix array. IEEE Trans Med Imaging 13.
Helfield B (2019) A review of phospholipid encapsulated ultrasound contrast agent microbubble physics. Ultrasound Med Biol 45:282–300.
Hingot V, Brodin C, Lebrun F, Heiles B, Chagnot A, Yetim M, Gauberti M, Orset C, Tanter M, Couture O, Deffieux T, Vivien D (2020) Early ultrafast ultrasound imaging of cerebral perfusion correlates with ischemic stroke outcomes and responses to treatment in mice. Theranostics 10:7480–7491.
Hobbs SK, Monsky WL, Yuan F, Roberts WG, Griffith L, Torchilin VP, Jain RK (1998) Regulation of transport pathways in tumor vessels: Role of tumor type and microenvironment. Proc Natl Acad Sci U S A 95:4607–4612.
Hu C-M-J, Zhang L, Aryal S, Cheung C, Fang RH, Zhang L (2011) Erythrocyte membrane-camouflaged polymeric nanoparticles as a biomimetic delivery platform. Proc Natl Acad Sci U S A 108:10980–10985.
Hurt RC, Wong K, Sawyer DP, Deshpande R, Mittelstein DR, Shapiro MG, Improved Acoustic Reporter Genes for Sensitive and Specific Imaging of Gene Expression, 26th European symposium on Ultrasound Contrast Imaging, Rotterdam, 2021.
Imbault M, Chauvet D, Gennisson J-L, Capelle L, Tanter M (2017) Intraoperative functional ultrasound imaging of human brain activity. Sci Rep 7:7304.
Ivanov KP, Kalinina MK, Levkovich YI (1981) Blood flow velocity in capillaries of brain and muscles and its physiological significance. Microvasc Res 22:143–155.
Kaufmann BA, Lindner JR (2007) Molecular imaging with targeted contrast ultrasound. Curr Opin Biotechnol 18:11–16.
Kaul S (2008) Myocardial contrast echocardiography. Circulation 118:291–308.
Keller D, Erö C, Markram H (2018) Cell densities in the mouse brain: A systematic review. Front Neuroanat 12.
Kirst C, Skriabine S, Vieites-Prado A, Topilko T, Bertin P, Gerschenfeld G, Verny F, Topilko P, Michalski N, Tessier-Lavigne M, Renier N (2020) Mapping the fine-scale organization and plasticity of the brain vasculature. Cell 180:780–795.e25.
Kosareva A, Abou-Elkacem L, Chowdhury S, Lindner JR, Kaufmann BA (2020) Seeing the invisible—ultrasound molecular imaging. Ultrasound Med Biol 46:479–497.
Lakshmanan A, Farhadi A, Nety SP, Lee-Gosselin A, Bourdeau RW, Maresca D, Shapiro MG (2016) Molecular engineering of acoustic protein nanostructures. ACS Nano 10:7314–7322.
Lakshmanan A, Jin Z, Nety SP, Sawyer DP, Lee-Gosselin A, Malounda D, Swift MB, Maresca D, Shapiro MG (2020) Acoustic biosensors for ultrasound imaging of enzyme activity. Nat Chem Biol 16:988–996.
Leow CH, Bazigou E, Eckersley RJ, Yu ACH, Weinberg PD, Tang M-X (2015) Flow velocity mapping using contrast enhanced high-frame-rate plane wave ultrasound and image tracking: methods and initial in vitro and in vivo evaluation. Ultrasound Med Biol 41:2913–2925.
Li B, Aid-Launais R, Labour M-N, Zenych A, Juenet M, Choqueux C, Ollivier V, Couture O, et al. (2019) Functionalized polymer microbubbles as new molecular ultrasound contrast agent to target P-selectin in thrombus. Biomaterials 194:139–150.
Lin F, Shelton SE, Espíndola D, Rojas JD, Pinton G, Dayton PA (2017) 3-D ultrasound localization microscopy for identifying microvascular morphology features of tumor angiogenesis at a resolution beyond the diffraction limit of conventional ultrasound. Theranostics 7:196–204.
Lin MZ, Schnitzer MJ (2016) Genetically encoded indicators of neuronal activity. Nat Neurosci 19:1142–1153.
Ling B, Lee J, Maresca D, Lee-Gosselin A, Malounda D, Swift MB, Shapiro MG (2020) Biomolecular ultrasound imaging of phagolysosomal function. ACS Nano 14:12210–12221.
Macé E, Montaldo G, Cohen I, Baulac M, Fink M, Tanter M (2011) Functional ultrasound imaging of the brain. Nat Methods 8:662–664.
Mace E, Montaldo G, Osmanski B-F, Cohen I, Fink M, Tanter M (2013) Functional ultrasound imaging of the brain: theory and basic principles. IEEE Trans Ultrason Ferroelectr Freq Control 60:492–506.
Maeda H, Bharate GY, Daruwalla J (2009) Polymeric drugs for efficient tumor-targeted drug delivery based on EPR-effect. Eur J Pharm Biopharm 71:409–419.
Maresca D, Correia M, Villemain O, Bizé A, Sambin L, Tanter M, Ghaleb B, Pernot M (2018a) Noninvasive imaging of the coronary vasculature using ultrafast ultrasound. JACC Cardiovasc Imaging 11:798–808.
Maresca D, Lakshmanan A, Abedi M, Bar-Zion A, Farhadi, A, Lu GJ, Szablowski JO, Wu D, Yoo S, Shapiro MG (2018b) Biomolecular Ultrasound and Sonogenetics. Annu Rev Chem Biomol Eng 9:229–252.
Maresca D, Lakshmanan A, Lee-Gosselin A, Melis JM, Ni Y-L, Bourdeau RW, Kochmann DM, Shapiro MG (2017) Nonlinear ultrasound imaging of nanoscale acoustic biomolecules. Appl Phys Lett 110:073704.
Maresca D, Payen T, Lee-Gosselin A, Ling B, Malounda D, Demené C, Tanter M, Shapiro MG (2020) Acoustic biomolecules enhance hemodynamic functional ultrasound imaging of neural activity. NeuroImage 209:116467.
Maresca D, Sawyer DP, Renaud G, Lee-Gosselin A, Shapiro MG (2018c) Nonlinear X-wave ultrasound imaging of acoustic biomolecules. Phys Rev X 8:041002.

Maresca D, Tanter M, Pernot M (2014) Ultrasound microangiography of the metacarophalangeal joint using ultrafast Doppler. In: 2014 IEEE International Ultrasonics Symposium (IUS). IEEE. p. 425–427.
Masamoto K, Kanno I (2012) Anesthesia and the quantitative evaluation of neurovascular coupling. J Cerebr Blood Flow Metab 32:1233–1247.
McGarry MP, Protheroe CA, Lee JJ (2010) Mouse hematology. Cold Spring Harbor Laboratory Press.
Moestue SA, Gribbestad IS, Hansen R (2012) Intravascular targets for molecular contrast-enhanced ultrasound imaging. Int J Mol Sci 13:6679–6697.
Montaldo G, Tanter M, Bercoff J, Benech N, Fink M (2009) Coherent plane-wave compounding for very high frame rate ultrasonography and transient elastography. IEEE Trans Ultrason Ferroelectr Freq Control 56:489–506.
Muleki-Seya P, Xu K, Tanter M, Couture O (2020) Ultrafast radial modulation imaging. IEEE Trans Ultrason Ferroelectr Freq Control 67:598–611.
Nakatsuka MA, Mattrey RF, Esener SC, Cha JN, Goodwin AP (2012) Aptamer-crosslinked microbubbles: smart contrast agents for thrombin-activated ultrasound imaging. Adv Mater 24:6010–6016.
Ohlendorf R, Wiśniowska A, Desai M, Barandov A, Slusarczyk AL, Li N, Jasanoff A (2020) Target-responsive vasoactive probes for ultrasensitive molecular imaging. Nat Commun 11:2399.
Ophir J, Parker KJ (1988), Contrast agents in diagnostic ultrasound. 15.
Pellow C, Tan J, Chérin E, Demore CEM, Zheng G, Goertz DE (2021) High frequency ultrasound nonlinear scattering from porphyrin nanobubbles. Ultrasonics 110:106245.
Pochon S, Tardy I, Bussat P, Bettinger T, Brochot J, von Wronski M, Passantino L, Schneider M (2010) BR55: A lipopeptide-based VEGFR2-targeted ultrasound contrast agent for molecular imaging of angiogenesis. Invest Radiol 45:89–95.
Rabut C, Correia M, Finel V, Pezet S, Pernot M, Deffieux T, Tanter M (2019) 4D functional ultrasound imaging of whole-brain activity in rodents. Nat Methods 16:994–997.
Rabut C, Yoo S, Hurt RC, Jin Z, Li H, Guo H, Ling B, Shapiro MG (2020) Ultrasound technologies for imaging and modulating neural activity. Neuron 108:93–110.
Schneider M, Anantharam B, Arditi M, Bokor D, Broillet A, Bussat P, Fouillet X, Frinking P, Tardy I, Terrettaz J, Senior R, Tranquart F (2011) BR38, a new ultrasound blood pool agent. Invest Radiol 46 (8):486–494.
Schneider M, Arditi M, Barrau M-B, Brochot J, Broillet A, Ventrone R, Yan F (1995) BR1: a new ultrasonographic contrast agent based on sulfur hexafluoride-filled microbubbles. Invest Radiol 30.
Schneider M, Broillet A, Bussat P, Giessinger N, Puginier J, Ventrone R, Yan F (1997) Gray-scale liver enhancement in VX2 tumor-bearing rabbits using BR14, a new ultrasonographic contrast agent. Invest Radiol 32:410–417.
Schumann PA, Christiansen JP, Quigley RM, Mccreery TP, Sweitzer RH, Unger EC, Lindner JR, Matsunaga TO (2002) Targeted-microbubble binding selectively to GPIIb IIIa receptors of platelet thrombi. Invest Radiol 37:587–593.
Segers T, Kruizinga P, Kok MP, Lajoinie G, de Jong N, Versluis M (2018) Monodisperse versus polydisperse ultrasound contrast agents: non-linear response, sensitivity, and deep tissue imaging potential. Ultrasound Med Biol 44:1482–1492.
Sehgal CM, Greenleaf JF (1984) Scattering of ultrasound by tissues. Ultrason Imaging 6:60–80.
Shapiro MG, Goodwill PW, Neogy A, Yin M, Foster FS, Schaffer DV, Conolly SM (2014) Biogenic gas nanostructures as ultrasonic molecular reporters. Nat Nanotechnol 9:311–316.
Shih R, Bardin D, Martz TD, Sheeran PS, Dayton PA, Lee AP (2013) Flow-focusing regimes for accelerated production of monodisperse drug-loadable microbubbles toward clinical-scale applications. Lab Chip 13:4816.
Siepmann M, Schmitz G, Bzyl J, Palmowski M, Kiessling F, Imaging tumor vascularity by tracing single microbubbles (2011) Imaging tumor vascularity by tracing single microbubbles. In: IEEE International Ultrasonics Symposium (IUS). IEEE. p. 1906–1909.
Soloukey S, Vincent AJPE, Satoer DD, Mastik F, Smits M, Dirven CMF, Strydis C, Bosch JG, et al. (2020), Functional ultrasound (fUS) during awake brain surgery: the clinical potential of intra-operative functional and vascular brain mapping. Front Neurosci 13:1384.
Song P, Manduca A, Trzasko JD, Chen S (2017a) Ultrasound small vessel imaging with block-wise adaptive local clutter filtering. IEEE Trans Med Imaging 36:251–262.
Song P, Trzasko JD, Manduca A, Huang R, Kadirvel R, Kallmes DF, Chen S (2018) Improved super-resolution ultrasound microvessel imaging with spatiotemporal nonlocal means filtering and bipartite graph-based microbubble tracking. IEEE Trans Ultrason Ferroelectr Freq Control 65:149–167.
Song W, Luo Y, Zhao Y, Liu X, Zhao J, Luo J, Zhang Q, Ran H, Wang Z, Guo D (2017b) Magnetic nanobubbles with potential for targeted drug delivery and trimodal imaging in breast cancer: an *in vitro* study. Nanomedicine 12:991–1009.
Szabo TL (2004) Diagnostic ultrasound imaging: inside out. Academic Press.
Talu E, Hettiarachchi K, Zhao S, Powell RL, Lee AP, Longo ML, Dayton PA (2007), Tailoring the size distribution of ultrasound contrast agents: possible method for improving sensitivity in molecular imaging. Mol Imaging 6:7290.2007.00034.
Tanter M, Fink M (2014) Ultrafast imaging in biomedical ultrasound. IEEE Trans Ultrason Ferroelectr Freq Control 61:102–119.
ten Kate GL, Renaud GGJ, Akkus Z, van den Oord SCH, ten Cate FJ, Shamdasani V, Entrekin RR, Sijbrands EJG, et al. (2012) Far-wall pseudoenhancement during contrast-enhanced ultrasound of the carotid arteries: clinical description and in vitro reproduction. Ultrasound Med Biol 38:593–600.
Tremblay-Darveau C, Williams R, Milot L, Bruce M, Burns PN (2016) Visualizing the tumor microvasculature with a nonlinear plane-wave doppler imaging scheme based on amplitude modulation. IEEE Trans Med Imaging 35:699–709.
Tsien RY (1998) The green fluorescent protein. Annu Rev Biochem 67:509–544.
Unger E, Shen D, Fritz T, Kulik B, Lund P, Wu G-L, Yellowhair D, Ramaswami R, et al. (1994) Gas-filled lipid bilayers as ultrasound contrast agents. Invest Radiol 29:S134–S136.
van Raaij ME, Lindvere L, Dorr A, He J, Sahota B, Foster FS, Stefanovic B (2011) Functional micro-ultrasound imaging of rodent cerebral hemodynamics. NeuroImage 58:100–108.
van Raaij ME, Lindvere L, Dorr A, He J, Sahota B, Foster FS, Stefanovic B (2012) Quantification of blood flow and volume in arterioles and venules of the rat cerebral cortex using functional micro-ultrasound. NeuroImage 63:1030–1037.
Walsby AE (1994), Gas vesicles. Microbiol Rev 58:94-144.
Wang LV, Yao J (2016) A practical guide to photoacoustic tomography in the life sciences. Nat Methods 13:627–638.
Wang S, Hossack JA, Klibanov AL (2018) Targeting of microbubbles: contrast agents for ultrasound molecular imaging. J Drug Target 26:420–434.
Wang X, Hagemeyer CE, Hohmann JD, Leitner E, Armstrong PC, Jia F, Olschewski M, Needles A, Peter K, Ahrens I (2012) Novel single-chain antibody-targeted microbubbles for molecular ultrasound imaging of thrombosis: validation of a unique noninvasive method for rapid and sensitive detection of thrombi and monitoring of success or failure of thrombolysis in mice. Circulation 125:3117–3126.
Willmann JK, Lutz AM, Paulmurugan R, Patel MR, Chu P, Rosenberg J, Gambhir SS (2008) Dual-targeted contrast agent for US assessment of tumor angiogenesis in vivo. Radiology 248:936–944.
Yang Y, Qiu Z, Hou X, Sun L (2017) Ultrasonic characteristics and cellular properties of anabaena gas vesicles. Ultrasound Med Biol 43:2862–2870.
Yu FT, Armstrong JK, Tripette J, Meiselman HJ, Cloutier G (2011), A local increase in red blood cell aggregation can trigger deep vein

thrombosis: evidence based on quantitative cellular ultrasound imaging. J Thromb Haemostas 9:481–488.
Zhao F, Unnikrishnan S, Herbst EB, Klibanov AL, Mauldin FW, Hossack JA (2020) A targeted molecular localization imaging method applied to tumor microvasculature. Invest Radiol 56:197–206.

(Received 16 November 2020, Accepted 5 March 2021)
(Available online 13 March 2021)